Materials Letters 63 (2009) 1455–1458

Contents lists available at ScienceDirect

Materials Letters

journal homepage: www.elsevier.com/locate/matlet

Two-step sintering of dense, nanostructural forsterite

M.H. Fathi *, M. Kharaziha

Department of Materials Engineering, Isfahan University of Technology, Isfahan, 8415683111, Iran

ARTICLE INFO

Article history:
Received 21 January 2009
Accepted 14 March 2009
Available online 29 March 2009

Keywords:
Ceramic
Nanomaterials
Sintering
Mechanical properties

ABSTRACT

This paper investigates a method for preparing the nanocrystalline forsterite dense ceramic via sintering the forsterite nanopowder. The two-step sintering (TSS) method has been applied to suppress the accelerated grain growth of forsterite nanopowder compacts. The effects of sintering parameters on the mechanical properties and the microstructure characteristics of the forsterite ceramic were studied. Results verified the applicability of this method to suppress the final stage of grain growth in the system. The grain size of the high density compacts (~98.5% TD) of the forsterite was 60–75 nm. The optimal hardness (940 Hv) and fracture toughness (3.61 MPa.m$^{1/2}$) of the prepared nanocrystalline forsterite were found to be higher than those of the currently available hydroxyapatite bioceramics. It was concluded that the two-step sintering method can be used to fabricate improved forsterite dense ceramics with desired bioactivity and mechanical properties that might be suitable for hard tissue repair and biomedical applications.

1. Introduction

Bioceramics have attracted increasing attention as replacements for structural components of the skeletal system due to their good biocompatibility. However, their poor mechanical properties such as brittleness and low fracture toughness restrict their use in load-bearing applications [1].

The forsterite (Mg_2SiO_4) ceramic is a new bioceramic with good biocompatibility [2]. Compared with hydroxyapatite ceramics, forsterite shows a significant improvement in the fracture toughness, superior to the lower limit reported for cortical bone [1,2].However, the sintering temperature of forsterite is too high, which impoverishes its mechanical properties [2,3].

Reduced grain size below 100 nm leads to the formation of nanostructured ceramics having superior mechanical properties [4]. In addition, the nanometer-sized grains and the high-volume fraction of grain boundaries in nanostructured materials have been found to increase osteoblast adhesion, proliferation, and mineralization [5,6]. However, fabrication of fully dense nanostructured ceramics is not easy. An accelerated grain growth during densification of nanopowder has been reported to deteriorate the advantages of nanostructured ceramics [7]. The two-step sintering (TSS) is an approach to controlling grain growth. This technique is used to suppress the accelerated grain growth that usually occurs during the final firing stage [7]. High-temperature heating followed by structural freezing via rapid cooling to a constant temperature levels off the grain growth but does not stop the densification.

In this research, fabrication of bulk dense nanocrystalline forsterite ceramics using the TSS method was studied in an attempt to obtain the optimum nanocrystalline forsterite with optimal mechanical properties.

2. Experimental procedures

The high-purity forsterite nanopowders required for our purposes in this study were synthesized by mechanical activation and heat treatment processes according to the methods described in the literature [8,9]. Morphological study was performed by transmission electron microscopy. Phase analysis and peak broadening determination of samples were performed using the X-ray diffraction technique.

The as-synthesized nanopowders were milled in a ball mill and mixed with 6 wt.% polyvinyl alcohol solution as the binder. The binder-to-powder ratio was optimized at 5/95 (w/w). Green compacts with an approximate density of 53 ± 2% of the theoretical density (TD) were formed by uniaxially pressing of the mixture at 550 MPa in a cylindrical mould. Sintering of the green bodies was carried out by two-step sintering methods. TSS processes were run by heating the samples up to 600 °C and retained for 60 min at this temperature. The specimens were then heated up to T1 (T1 = 1100–1300 °C). After retention for 6 min at T1, the specimens were cooled down to T2 (T2 = 750 and 850 °C) and subsequently kept in the second step temperature for 2–15 h. The heating rate of TSS was 10 °C min^{-1}. The cooling rate of TSS, between T1 and T2, was 50 °C min^{-1} and after T2, it was 10 °C min^{-1}.

Scanning electron microscopy (SEM) was used to study the fracture surface of forsterite ceramics. To investigate the grain growth during sintering and after full densification, the sintered pellet was mechanically polished and etched. Microhardness of each sample was

* Corresponding author. Tel.: +98 311 3915708; fax: +98 311 3912752.
E-mail address: fathimoh@yahoo.com (M.H. Fathi).

0167-577X/$ – see front matter © 2009 Elsevier B.V. All rights reserved.
doi:10.1016/j.matlet.2009.03.040

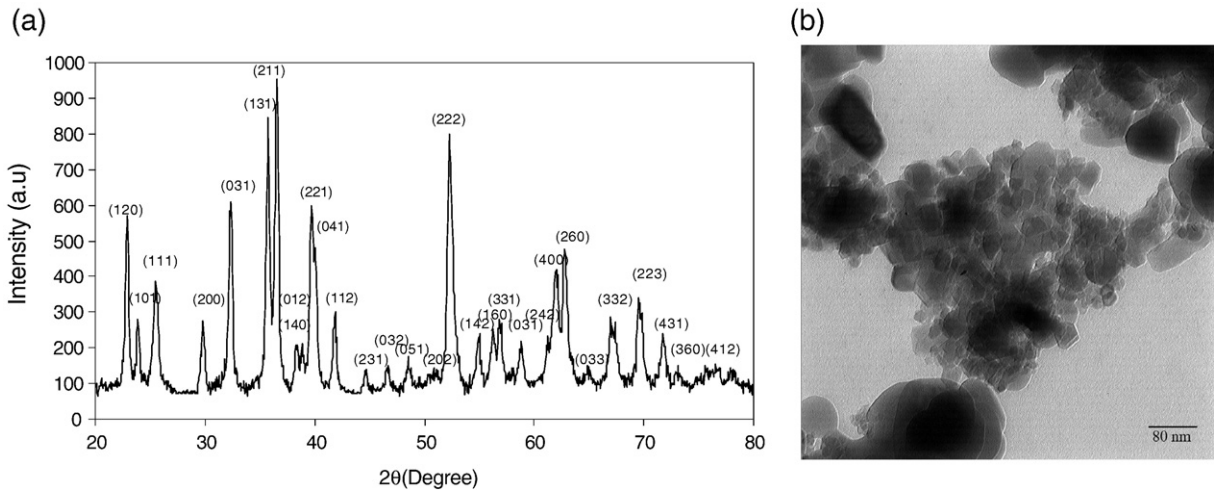

Fig. 1. (a) XRD pattern and (b) TEM micrographs of forsterite nanopowder.

tested using the Vickers indentation technique applying a loading of 9.8 N and a dwell time of 15 s. The fracture toughness was determined using the direct crack measurement method according to Niihara's formula [10].

3. Results and discussion

Fig. 1(a) shows the XRD pattern of the prepared forsterite nanopowder after 10 h mechanical activation and heat treatment at 1200 °C for 1 h. The nanopowders were characterized by highly crystalline and no second phases. The grain size of the prepared forsterite at the mentioned temperature was about 30–57 nm as revealed by the XRD line-broadening technique and using the Williamson–Hall's equation [11]. The morphology of the prepared forsterite nanopowder is shown in Fig. 1(b). It is obvious that the forsterite nanopowder exhibits agglomerative morphologies with irregular shape and width dispense of particle sizes (20–60 nm).

Fig. 2 shows the effect of the first step temperature of the TSS process on the densification of the specimens. It is seen that sufficiently high density has been obtained during the first stages (0 h-curve) (73–80%TD). During the second step, densities improved from a lower value to higher than 98.5%TD. Under the TSS regime ($T1 \leq 1150$ °C) with prolonged soaking up to 15 h, no tangible variation was observed in density. Densification occurred when the distances between the centers of the crystallites diminished, which required an off-transport of matter from the grain boundaries to the neck. This was impossible without volume and grain boundary diffusion. At these temperatures ($T1 \leq 1150$ °C), densification mechanisms such as grain boundary and volume diffusion were not active; so, densification was exhausted.

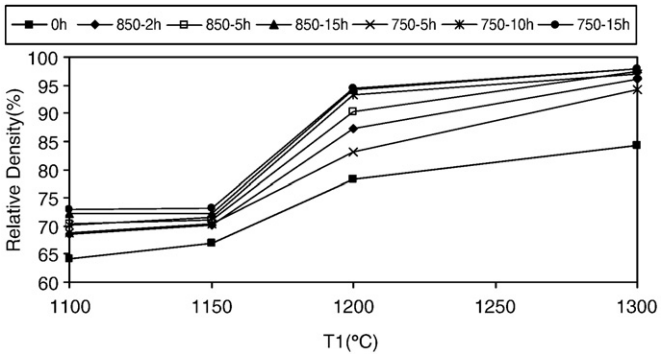

Fig. 2. Relative density of forsterite compacts as a function of the TSS first step temperature.

Mazaheri et al. [12] reported that there exists a critical temperature of the second step for nanocrystalline materials to derive a full density structure without grain growth. The TSS regime carried out with a second step temperature (T2) below the critical one turned out to be a disappointing process.

When T1 of up to 1200 °C was selected, relative density increased by increasing the holding time and the TSS second step temperature. Under these conditions, the residual pores after the first step of TSS must be subcritical and unstable against shrinkage. Results of the TSS process show that the critical density making pores unstable at the end of the first step was around 78.2%TD.

Fig. 3(a) shows grain size versus relative density of the samples sintered at TSS regime ($T1 = 1300$ °C and $T2 = 750$ °C (named TSS1)) and at TSS regime ($T1 = 1300$ °C and $T2 = 850$ °C (named TSS2)). Soaking of the samples under the TSS1 regime led to a significant densification (from 84%TD to 98.5%TD), while no significant increase occurred in the grain size. In contrast, a significant increase occurred in grain size when the TSS2 regime was used, although a fully dense ceramic was obtained after 15 h soaking time at TSS second step. Chen [7] suggests that for achieving densification without a significant grain growth, grain boundary diffusion needs to remain active, while the grain boundary migration is to be suppressed. A mechanism to slow down the grain boundary movement is the triple-point drag. Grain growth entails a competition between grain boundary mobility and junction mobility. Once the latter becomes less, particularly at low temperatures in which junctions are rather immobile, the mentioned drag would occur. The grain growth prohibition is, therefore, achievable under the above circumstances. This grain boundary diffusion accompanied by the so-called triple-point drag at low temperatures (T2) prepares a full density microstructure with a constant grain size. For the forsterite ceramic, $T2 = 850$ °C might be too high to immobilize the grain boundary and the best condition for the TSS processing of the forsterite nanopowder is the TSS1 regime with soaking at 750 °C up to 15 h. Under such conditions, the grain size of the forsterite ceramic was estimated by the Scherer's formula [13] at about 60–75 nm, which shows that densification was achieved without grain growth.

Fig. 3(b) shows the SEM micrograph of the fracture surface of the forsterite ceramic sintered under TSS1 process for 15 h soaking time at TSS second step. Well-defined grains are visible with almost negligible porosity. The micrograph of the fracture surface of the forsterite shows

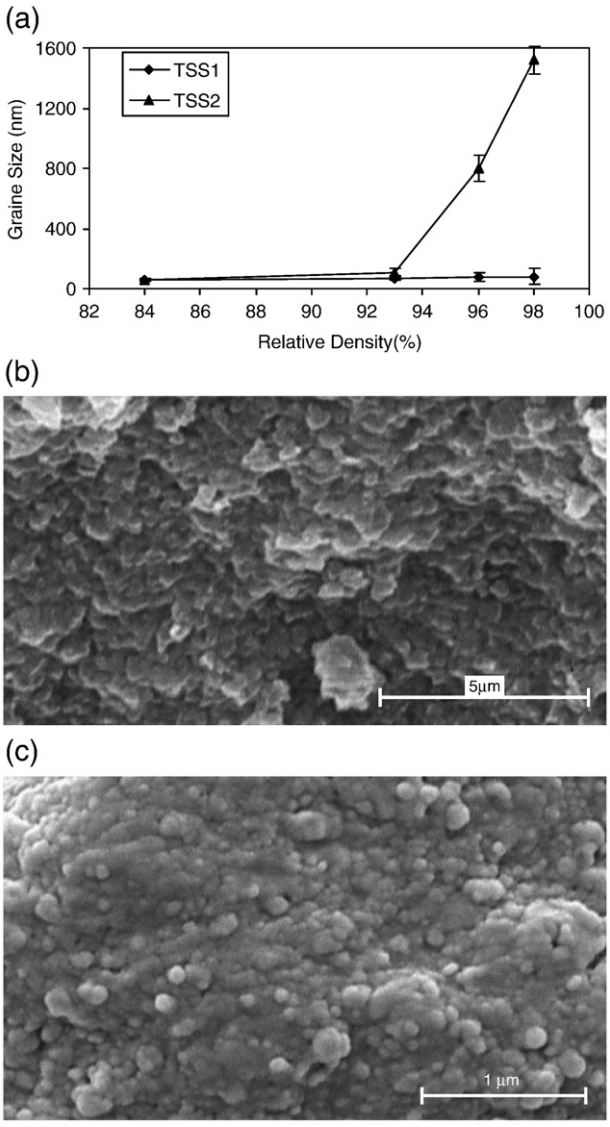

Fig. 3. (a) Average grain size versus fractional density of forsterite compacts sintered under TSS process, SEM micrographs of (b) fracture surface and, (c) surface of forsterite compact sintered according to TSS1 process.

intergranular fracture, uniform grain size distribution, and no abnormal grain growth. Fig. 3(c) shows the SEM micrograph of surface of the forsterite ceramic sintered under TSS1 process for 15 h soaking time at TSS second step. The bimodal grain size distribution shows the small grain range below 300 nm.

Fig. 4 shows hardness (Fig. 4(a)) and fracture toughness (Fig. 4(b)) of forsterite compacts sintered by two regimes according to the relative density. It is observed that the hardness and fracture toughness values vary from 450 to 940 Hv and 1.5 to 3.61 MPa $m^{1/2}$ which more appropriately reflects the sintering degree when compare to %TD (~75–98.6%). The standard deviation of hardness and fracture toughness values may also provide useful information about the sintering degree. The hardness and fracture toughness noticeably deviate for test piece at initial and intermediate sintering stage as the porosity level is high. If the surface underneath the indentation consist porosity that weaken the test surface, the indentation mark becomes bigger and will cause low hardness reading.

As can be seen, under TSS regime (T2 = 750 °C and holding time = 15 h) fracture toughness and hardness of forsterite compacts increased to 3.61 ± 0.1 MPa $m^{1/2}$ and 940 ± 10 Hv, respectively, by increasing the relative density (up to 98%TD). Although under the TSS regime (T2 = 850 °C and holding time = 15 h) with a prolonged the first step temperature (up to 1300 °C) full density was observed (Fig. 2), the results showed that hardness and fracture toughness declined. According to the grain size of forsterite ceramic in Fig. 3, these could be due to grain coarsening after prolonging sintering at elevated temperature.

Ni et al. [2] prepared a forsterite ceramic (92.5%TD) from a coarse grain forsterite powder by 8 h of sintering at 1450 °C with a fracture toughness of about 2.4 MPa $m^{1/2}$[2]. According to Figs. 3 and 4, the fracture toughness of the sintered forsterite was increased to 3.61 ± 0.1 MPa $m^{1/2}$ with grain size reduction to about 60–75 nm. As it can be seen the mechanical properties of forsterite ceramic is closely related with their microstructures, i.e. grain size, porosity, grain boundary and, etc. Generally, hardness and fracture toughness of ceramics increase with decreasing of porosity and grain size. There are several researches available, reporting a superior strength and higher fracture toughness for finer microstructures in comparison with coarser ones [12,14]. For instance, Ramesh et al. [15] have found the fracture toughness of HA ceramics with the grain sizes of around 2.1 and 0.2 μm to be ~0.96 and ~1.45 MPa $m^{1/2}$, respectively.

In comparison to the hydroxyapatite ceramics (K_{IC} = 0.75–1.2 MPa $m^{1/2}$ and hardness = 700 Hv) [1,2], the results of this study suggest that the nanocrytalline forsterite dense ceramics can be significantly improved with regards to their fracture toughness (K_{IC} = 3.61 MPa. $m^{1/2}$) and hardness (Hv = 940 Hv). In addition, nanostructured bioceramics are expected to have better bioactivity than coarser crystals. Thus, the nanocrystalline forsterite dense bioceramic fabricated in this study not only exhibited better mechanical properties compared to other bioceramics, but it also possessed improved biocompatibility and bioactivity which might make it suitable for hard tissue repair and biomedical applications.

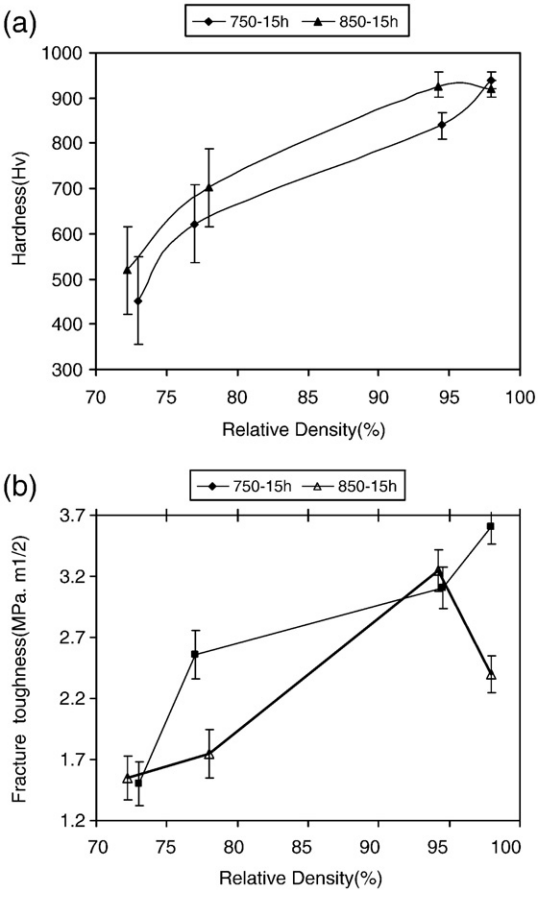

Fig. 4. (a) Vickers hardness, and (b) fracture toughness of forsterite as a function of relative density (%).

4. Conclusions

Applicability of the two-step sintering method for preparing nanocrystalline forsterite dense ceramics using the forsterite nanopowder was investigated. Using the TSS conducted at T1 = 1300 °C (for 6 min) and T2 = 750 °C (for 15 h), full density nanocrystalline forsterite ceramics (~98.5%TD) were fabricated with fracture toughness and microhardness values of about 3.61 ± 0.1 MPa $m^{1/2}$ and 940 ± 10 Hv, respectively. The grain size of the nanocrystalline forsterite obtained was about 60–75 nm. In conclusion, an improved nanostructured forsterite dense ceramic was prepared which possesses the desired bioactivity and mechanical properties and might be suitable for hard tissue repair and biomedical applications.

Acknowledgment

The authors are grateful for the support of this research by Isfahan University of Technology.

References

[1] Knepper M, Moricca S, Milthorpe BK. Biomaterials 1997;18:1523–9.
[2] Ni S, Chou L. Ceram Int 2007;33:83–8.
[3] Song KX, Chen XM. Mater Lett 2008;62:520–2.
[4] Cottom BA, Mayo MJ. Scr Mater 1996;34:809–14.
[5] Catledge SA, Fries MD, Vohra YK, Lacefield WR. J Nanosci Nanotechnol 2008;2:293–312.
[6] Webster TJ, Ergun C, Dormers RH, Siegel RW, Bizios R. Biomaterials 2000;21:1803–10.
[7] Wang XH, Chen PL, Chen IW. J Am Ceram Soc 2006;89:431–7.
[8] Fathi MH, Kharaziha M. Mater Lett 2008;62:4306–9.
[9] Fathi MH, Kharaziha M. J Alloys Compd 2009;472:540–5.
[10] Niihara K. Ceramic 1985;20:1218.
[11] Williamson K, Hall WH. Acta Metall 1953;1:22–31.
[12] Mazaheri M, Valefi M, Razavi Hesabi Z, Sadrnezhaad SK. Ceram Int 2009;35:13–20.
[13] Cullity BD, Stock SR. Elements of X-Ray Diffraction. 3rd ed. New Jersey, Prentice Hall, 2001.
[14] Armstrong RW. Int J Refract Met Hard Mater 2001;19:251–5.
[15] Ramesh S, Tan CY, Sopyan I, Hamdi M, Teng WD, Teng WD. Adv Mater 2007;8:124–30.